

OZONE PROFILES AND TROPOSPHERIC OZONE FROM GLOBAL OZONE MONITORING EXPERIMENT

X. Liu⁽¹⁾, K. Chance⁽¹⁾, C.E. Sioris⁽¹⁾, R.J.D. Spurr⁽¹⁾, T.P. Kurosu⁽¹⁾, R.V. Martin⁽²⁾, M.J. Newchurch⁽³⁾, P.K. Bhartia⁽⁴⁾

⁽¹⁾Atomic and Molecular Physics Division, Harvard-Smithsonian Center for Astrophysics, 60 Garden Street, Cambridge, MA, USA, Email: xliao@cfa.harvard.edu; kchance@cfa.harvard.edu

⁽²⁾Department of Physical and Atmospheric Sciences, Dalhousie University, Halifax, NS, Canada

⁽³⁾Atmospheric Science Department, University of Alabama in Huntsville, Huntsville, Alabama, USA

⁽⁴⁾Atmospheric Chemistry and Dynamics Branch, NASA GSFC, Greenbelt, Maryland, USA

ABSTRACT

Ozone profiles are derived from backscattered radiances in the ultraviolet spectra (290-340 nm) measured by the nadir-viewing Global Ozone Monitoring Experiment using optimal estimation. Tropospheric O₃ is directly retrieved with the tropopause as one of the retrieval levels. To optimize the retrieval and improve the fitting precision needed for tropospheric O₃, we perform extensive wavelength and radiometric calibrations and improve forward model inputs. Retrieved O₃ profiles and tropospheric O₃ agree well with coincident ozonesonde measurements, and the integrated total O₃ agrees very well with Earth Probe TOMS and Dobson/Brewer total O₃. The global distribution of tropospheric O₃ clearly shows the influences of biomass burning, convection, and air pollution, and is generally consistent with our current understanding.

1. INTRODUCTION

The retrieval of O₃ profile including the troposphere from Global Ozone Monitoring Experiment (GOME) has been demonstrated in recent years using physics-based approaches [1-4]. These algorithms require very accurate radiometric and wavelength calibrations, and accurate modeling of the atmosphere other than O₃, including clouds, aerosols, and temperature profiles.

This study performs detailed wavelength and radiometric calibrations, improves forward model inputs using our best available knowledge, and derives O₃ profiles and tropospheric O₃ from measured GOME radiances in the ultraviolet. We validate the retrievals against ozonesonde, Dobson/Brewer and TOMS measurements and present the global distribution of tropospheric O₃.

2. DATA AND METHODOLOGY

Ozone profile retrieval from nadir spectra is an ill-conditioned problem. Therefore, we choose the well-known Optimal Estimation (OE) technique for inversion [5]. OE uses available *a priori* knowledge to stabilize retrievals. Because the information content from nadir-viewing spectra

is limited, using proper *a priori* climatology is important. We use the TOMS V8 climatology as a *priori* and *a priori* variance. This climatology is month- and latitude-dependent and is derived from Stratospheric Aerosol and Gas Experiment (SAGE), Polar Ozone and Aerosol Measurement (POAM), and ozonesonde observations [6]. A correlation length of 6 km is used to construct the *a priori* covariance matrix.

We improve the wavelength and radiometric calibrations as follows. (1) We derive variable slit widths, and shifts between radiances/irradiance, at every 2-nm region with a high-resolution solar reference spectrum [7]. (2) Shifts between trace gas absorption cross-sections and radiances are fitted in the retrieval. (3) We perform on-line correction of the filling in of solar and telluric absorption features using Ring spectra calculated with a first-order rotational Raman scattering model [8]. Ring spectra are updated when total O₃ changes by ≥ 20 Dobson Units (DU). (4) Undersampling of GOME is corrected using a high-resolution solar reference spectrum [9]. (5) We improve the polarization correction to GOME measurements using the GOMECAL package [10] (http://www.knmi.nl/gome_fd/gomecal/).

We improve characterization of the atmosphere with cloud information from the GOME Cloud Retrieval Algorithm [11], monthly mean SAGE II aerosols [12] and GEOS-CHEM tropospheric aerosols [13]; daily European Centre for Medium-Range Weather Forecasts (ECMWF) temperature profiles (<http://www.ecmwf.int>) for extracting tropospheric O₃ from the temperature-dependent Huggins bands [14], and daily surface pressure from National Centers for Environmental Prediction/National Center for Atmospheric Research (NCEP/NCAR) reanalysis data (<http://www.cdc.noaa.gov>). Initial albedo is based on derived GOME surface albedo database [15]. Cloud fraction is readjusted from measured reflectance at 370.02 nm where absorption is minimal.

The retrieval uses measurements in the windows 290-307 nm and 327-336 nm. Measurements below 290 nm are not used because of large measurements errors and NO emission

lines. We also find that including band 1b measurements between 307 and 314 nm does not improve the retrievals probably because of inconsistent calibration with band 1a measurements. In addition, GOME slit function and wavelength shifts vary rapidly at the beginning of band 2b (312–327 nm), which makes it difficult to use them to improve the retrievals. The spatial resolution of retrievals is 960 km × 80 km.

Partial columns are typically retrieved on an 11-layer Umkehr-like grid except in the troposphere, where retrieval grids are modified using tropopause pressure and surface pressure. Besides the O₃ variables, the state vector includes an albedo parameter for band 1b, three albedo parameters for band 2b to account for its wavelength-dependence, four cross section shift parameters for each band, four wavelength shift parameters for each band, scaling and shift parameters for minor species (e.g., NO₂, SO₂, BrO), two parameters for undersampling correction, one Ring scaling parameter for band 1a, and three Ring scaling parameters for band 2b to account for multiple scattering, and three parameters to account for the degradation correction in band 1a. The degradation parameters are used only in band 1a because band 1a measurements are more severely degraded. The total O₃ information from band 2b implicitly constrains the degradation correction in band 1a.

We use LIDORT [16] to calculate radiances and weighting functions. The scalar radiances from LIDORT are corrected for neglecting polarization using a look up table.

The retrievals are compared with correlative TOMS V8 and Dobson/Brewer total O₃ measurements and ozonesonde observations. The equator crossing time difference between TOMS and GOME is approximately one hour. We use the gridded TOMS data (1.0° latitude × 1.25° longitude); all TOMS measurements (~ 20 values) within a GOME footprint are averaged. The coincident criteria for Dobson/Brewer and ozonesonde measurements are 1.5° degree in latitude, 600 km in longitude, and 8 hours. Ozonesonde measurements during 1996–2000 at 11 stations are used in these studies (Table 1). Six stations also have total O₃ measurements from the Dobson or Brewer measurements.

Table 1. List of ozonesonde stations (abbreviation name), locations, the time period during which data are used, and the availability and type of total O₃ (TOZ) measurements. The measurements at Scoresbysund are obtained from Network for the Detection of Stratospheric Change (NDSC, <http://www.ndsc.ncep.noaa.gov>). The measurements at Java are obtained from M. Fujiwa before 1998 and from Southern Hemisphere Additional Ozonesondes (SHADOZ) [17] since 1998. Other data are obtained from World Ozone and Ultraviolet Radiation Data Center (WOUDC, http://www.woudc.org/index_e.html).

Station (abbr.)	Location	Time	TOZ
Ny Ålesund (ny)	78.9°N, 11.9°E	96-00	N/A ¹
Scoresbysund (sc)	70.5°N, 22.0°W	96-00	N/A
Sodankylä (so)	67.4°N, 26.7°E	96-98	Brewer
Hohenpeißenberg (ho)	47.9°N, 11.0°E	96-00	Dobson
Hilo (hi)	19.6°N, 155°W	96-00	Dobson ²
Nairobi (nr)	1.3°S, 36.8°E	97-00	Dobson ³
Java (ja)	7.6°S, 112.7°E	96-00	N/A
Ascension (as)	8.0°S, 14.4°W	97-00	N/A
America Samoa (sa)	14.2°S, 170.6°W	96-00	Dobson
Lauder (la)	45.0°S, 169.7°E	96-00	Dobson
Neumayer (ne)	70.7°S, 8.3°W	96-00	N/A

1. Total O₃ is available only during 1996–1997 and is not used.
2. The total O₃ is measured at a close station Mauna Loa (19.5°N, 155.6°E); its surface altitude is 3.4 km.
3. Total O₃ is available only during 1997–1999.

3. RESULTS AND DISCUSSION

3.1. Comparisons with TOMS and Dobson/Brewer Total O₃

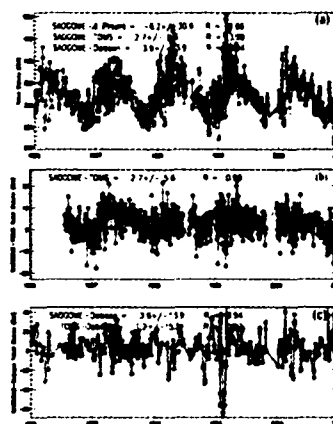


Fig. 1. Comparisons of integrated total O₃ (purple) with TOMS (red) and Dobson total O₃ (green) at Hohenpeißenberg. (a) Total O₃. (b) Difference between GOME and TOMS. (c) Difference between GOME/TOMS and Dobson. The *a priori* O₃ is also shown as yellow in (a).

Fig. 1a shows the time series of integrated total O₃ together with TOMS and Dobson total O₃ at Hohenpeißenberg. Their differences are shown in Fig. 1b and Fig. 1c. The time series of differences do not change with time, suggesting that band 2 measurements do not degrade much and the severe degradation in band 1a since 1998 [3] are well handled using the above-mentioned degradation correction scheme. We can see that our retrievals agree very well with both TOMS and Dobson total ozone with average biases less than 4 DU. Table 2 shows the biases, standard deviations, and correlation coefficients between our retrieved, TOMS, and Dobson/Brewer total O₃. The biases are within 7 DU at all stations; the correlation coefficients are greater than 0.92 between GOME and TOMS and greater than 0.87 between GOME and Dobson/Brewer. These biases are within the retrieval uncertainties of different retrievals and the spatiotemporal variability of total O₃. Compared to the *a priori*, we can certainly see significant improvements, with smaller biases and much smaller standard deviations. The standard deviations are

smaller for comparisons with TOMS measurements because of similar spatial domains. In the comparison with Dobson measurements, we are comparing area vs. point measurements; it is expected that the standard deviations will be larger. We note that the standard deviations are larger at higher latitudes because of larger spatiotemporal variability. For example in Fig. 1c, there are a few large differences, greater than 40 DU, between GOME/TOMS retrievals and Dobson measurements in the January and February of 1999. The longitude differences are greater than 5° and the time difference are greater than 4 hours. There are large spatial gradients over this region for these days as seen from TOMS data, suggesting that these large differences result from the large spatiotemporal O₃ variability at mid-latitudes in the winter and early spring.

Table 2. Biases, standard deviations, and correlation coefficients between GOME total O₃ and *A priori*/TOMS/Dobson/Brewer total O₃. The O₃ between retrieval surface to station surface altitude is taken into account in the following comparisons. The units for biases and standard deviations are DU.

Station	GOME- <i>A Priori</i>	GOME-TOMS	GOME-Dobson
ny	-23.3±39.0/0.66	-3.3±8.3/0.99	N/A
sc	-13.3±40.0/0.68	2.0±6.8/0.99	N/A
so	-29.3±41.0/0.53	0.0±7.8/0.99	-5.2±14.2/0.97
ho	-6.2±30.6/0.66	2.7±5.5/0.99	3.9±13.9/0.94
hi	-5.1±13.1/0.66	-2.3±4.2/0.97	0.8±6.3/0.95
nr	1.3±12.2/0.22	-1.5±4.8/0.93	-2.9±6.0/0.87
ja	-13.4±7.6/0.62	-5.6±3.8/0.92	N/A
as	1.8±8.2/0.59	0.2±3.7/0.94	N/A
sa	-9.8±8.3/0.54	-3.9±3.4/0.93	2.3±4.2/0.91
la	-8.5±23.2/0.80	-3.6±6.2/0.99	0.8±18.8/0.88
nc	-26.0±31.0/0.85	-6.3±7.9/0.99	N/A

3.2. Comparisons of O₃ profiles with ozonesonde

Because ozonesonde measures O₃ only up to ~35 km, we can only compare the bottom seven layers. We integrate the ozonesonde profiles to partial columns at each layer corresponding to their collocated GOME retrievals. In order to assess the accuracy of the GOME retrievals, the ozonesonde profiles are not convolved with retrieval averaging kernels because smoothing contributes to retrieval errors. Fig. 2 shows the comparison of retrieved O₃ profiles with ozonesonde measurements at Hohenpeißenberg. We can see that the retrievals agree very well with ozonesonde measurements. The average biases are within 2.5 DU and 10% at each layer (Fig. 3).

Fig. 3 shows the average biases and standard deviations between retrieved/*a priori* profiles and ozonesonde profiles. For Scoresbysund, Sodankylä, Hohenpeißenberg, and Lauder, the comparisons are very good with average biases within 6 DU and 15% at each layer. The standard deviations between retrievals and ozonesonde are usually

reduced relative to those between *a priori* and ozonesonde O₃.

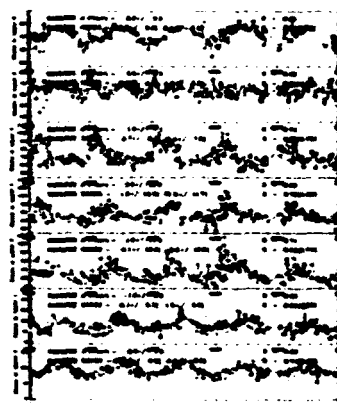


Fig. 2. Comparisons of GOME retrieved (purple circles) and ozonesonde O₃ profiles (green triangles) for the bottom seven layers (0~35 km) at Hohenpeißenberg. The *a priori* are shown as yellow.

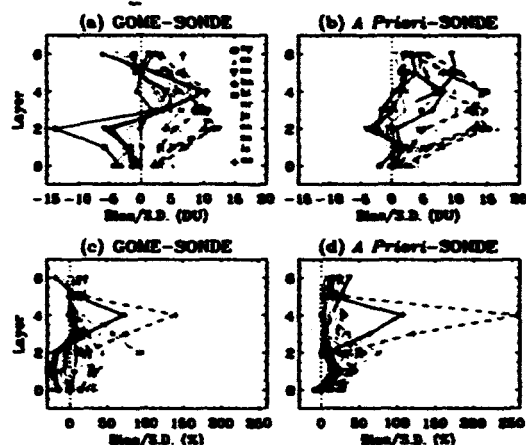


Fig. 3. Mean biases (solid) and standard deviations (dashed) at all stations for (a) GOME - sonde, (b) GOME *a priori* - sonde. (c) and (d) are similar to (a) and (b) except for relative biases and standard deviations.

At Ny Ålesund, there is generally good agreement except at for layer 2 (~10-15 km), where the mean bias is -13 DU, although the difference between *a priori* and ozonesonde is much smaller (-2.6 DU). This difference is usually larger during the spring than the summer, and is slightly correlated with solar zenith angle ($R=0.24$) and cloud fraction ($R=0.34$). The bias is probably due to the incorrect assignment of ice surface to clouds and is currently under investigation. At Neumayer, large biases occur at layer 4 (~20-25 km) with a mean bias of 10 DU. The relative bias can be greater than 200%, especially when there is strong O₃ depletion and the column O₃ is less than 10 DU. The bias is partly due to similar large bias in the *a priori* O₃. For the five tropical stations, the agreements are within 5 DU and 10% for layers 5 and 6 and are within 4 DU and 30% for layers 0 and 1, but large biases occur at layers 3, 4, and 5. Thompson et al. [17]

also reported large biases between TOMS and SHADOZ integrated and evaluated total O₃. Currently, our integrated total O₃ columns agree very well with Dobson and TOMS total O₃ columns. It is not clear whether these large biases result from retrieval errors or ozonesonde measurement errors. We notice that the biases for those layers at America Samoa and Hilo are actually much smaller before early 1998, when sensor solution for measurements was switched from 1% KI-buffered solution to 2% KI unbuffered solution.

3.3 Comparisons of tropospheric O₃ with ozonesonde

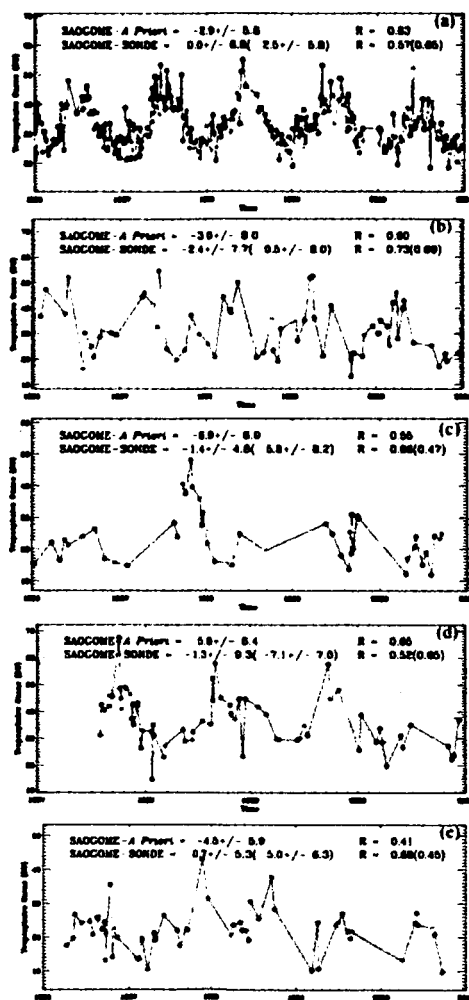


Fig. 4 Comparisons between GOME retrieved (purple circles) and ozonesonde (green triangles) tropospheric O₃ columns at (a) Hohenpeißenberg, (b) Hilo, (c) Java, (d) Ascension, and (e) American Samoa. The *a priori* are also shown as yellow.

Fig. 4 compares the integrated tropospheric O₃ column at five stations. We can see that our retrievals agree very well with ozonesonde measurements. Most of the small-scale variabilities are captured by our retrievals. For example, at Java, although the *a priori* values are usually around 30 DU, our retrievals successfully capture small values (~15 DU) as well as enhanced values (~50 DU) during the period of intense biomass burning resulting from 1997-1998 El Niño event. Table 3 summarizes the biases, standard deviations and correlation coefficients at all the stations. The average biases are usually within 3 DU and the standard deviations are within 9 DU except at Ny Ålesund, Scoresbysund, and Neumayer, where there are large biases. The large biases at those stations may result from the incorrect treatments of cloud and ice surface. There is a large standard deviation at Ascension Island, which is because the South Atlantic Anomaly can largely affect the retrieval.

Table 3. Biases, standard deviations and correlation coefficients between retrieved/*a priori* and ozonesonde tropospheric O₃. The units for biases and standard deviations are DU.

Station	GOME - SONDE	A Priori - SONDE
ny	-7.0±6.0/0.22	0.64±6.5/0.39
sc	-3.5±5.5/0.46	2.6±6.2/0.61
so	-2.0±5.4/0.59	2.7±6.1/0.59
ho	0.0±6.8/0.57	2.4±5.8/0.65
hi	-2.4±7.7/0.73	0.5±8.0/0.68
nr	-3.0±8.0/0.42	-1.8±5.4/0.29
ja	-1.4±4.8/0.86	5.8±8.2/0.47
as	-1.3±9.3/0.52	-7.13±7.0/0.65
sa	0.6±5.3/0.68	5.0±6.3/0.45
la	-1.4±6.4/0.10	-1.0±4.8/0.50
ne	-4.7±6.6/0.78	2.2±4.1/0.92

The retrieval errors in tropospheric O₃ due to random noise and smoothing are less than 3 DU for tropical regions and less than 5 DU for mid-latitude regions. The accuracy in ozonesonde measurements is 5-15% [18]. The natural tropospheric O₃ variability is 20-30% at mid-latitudes [19]; the tropospheric O₃ can change by a factor of 3 at most SHADOZ stations [20]. Considering the spatial and time domain difference and the spatiotemporal variability of tropospheric O₃, we can say that our retrievals are very consistent with ozonesonde measurements within the measurement/retrieval uncertainties and spatiotemporal variability.

3.4 Global distribution of tropospheric O₃

Fig. 5 (top) shows the global distribution of tropospheric O₃ during 2/24-26/1997. In the tropics, there is low O₃ over the Pacific Ocean, where there are intense convection activities. Over North Africa (~0°E, 10°N), a region with intense biomass burning during this period, there is enhanced tropospheric O₃, which is not presented in most of the tropospheric O₃ retrievals [21]. However, the O₃

values are smaller than those over the South Atlantic Ocean, consistent with the observed Atlantic tropospheric paradox [22]. In the Antarctic, the tropospheric O_3 is consistently less than 15 DU. Near $30^\circ N$ and $30^\circ S$, which corresponds to downward motion of Hadley circulation, there are bands of high tropospheric O_3 even over the ocean. These high O_3 values are probably due to the complex interplay of photochemistry and localized/transported pollution under favorable weather conditions. During 9/16-18/1997, the two bands of high O_3 and the low O_3 over Pacific Ocean with shift slightly north with the motion of intertropical convergence zone (ITCZ). There is enhanced tropospheric O_3 over Indonesia, consistent with the intense biomass burning and meteorological conditions (e.g. dry air, less precipitation) caused by the 1997-1998 El Niño event. Over South America, South Africa and the Atlantic Ocean, high O_3 values of 40-60 DU result from intense biomass burning over South Africa and South America.

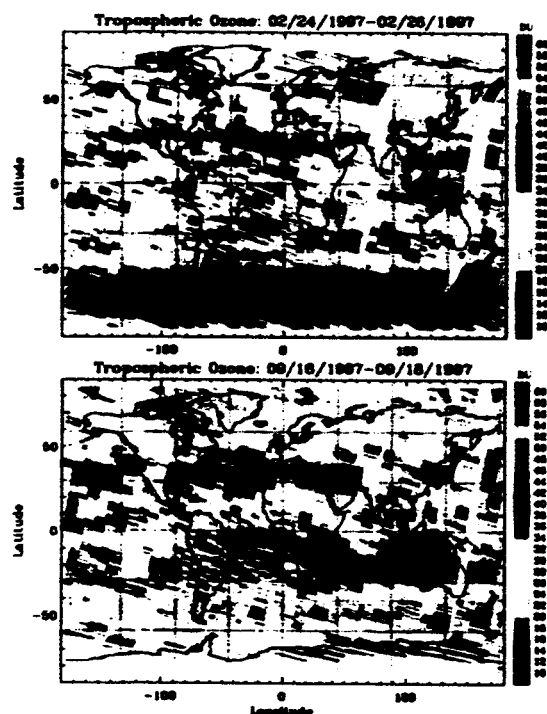


Fig. 5 Three-day composites of global distribution of tropospheric O_3 . (a) 2/24-26/1997. (b) 9/16-18/1997. The noisy patterns over the South Atlantic Ocean are caused by the South Atlantic Anomaly.

4. CONCLUSION

An algorithm was developed to retrieve O_3 profiles and tropospheric O_3 from GOME using the optimal estimation technique. We particularly focus on tropospheric O_3 derivation by performing extended wavelength and radiometric calibrations and improving forward model

inputs. Tropospheric O_3 is directly retrieved by using tropopause as one of the retrieval layers. We validate our retrievals against TOMS and Dobson/Brewer total O_3 and ozonesonde measurements at 11 high-latitude, mid-latitude, and tropical stations. The integrated total ozone agrees very well with TOMS and Dobson/Brewer measurements with average biases less than 7 DU. Retrieved O_3 profiles generally agree well with ozonesonde measurements except some large biases in the stratosphere at Ny Ålesund, Neumayer, and tropical stations. The large biases at Ny Ålesund and Neumayer may be related to the incorrect assignment of snow/ice surface to clouds. It is unclear whether the large biases at those tropical stations are due to ozonesonde measurement errors or our retrieval errors. The retrieved tropospheric O_3 columns agree very well with ozonesonde measurements except at Ny Ålesund and Neumayer, capturing most of low and high O_3 in the ozonesonde measurements. Global distributions of tropospheric O_3 are presented. They clearly show signals due to biomass burning, convection, air pollution, and transport and are generally consistent with our current knowledge and understanding.

Acknowledgements This study is supported by the NASA Atmospheric Chemistry and Modeling Analysis Program and by the Smithsonian Institution. We thank WUDC and its data providers, SHADOZ, NDSC, S.B. Anderson and M. Fujiwara for providing ozonesonde measurements. We also thank R. van Oss for providing his software and look-up tables for polarization correction.

References

1. Munro R., et al. Direct measurement of tropospheric ozone from space, *Nature*, 392, 168-171, 1998.
2. Hoogen R., et al. Ozone profiles from GOME satellite data: Algorithm description and first validation, *J. Geophys. Res.*, 104, 8263-8280, 1999.
3. van der A R.J., et al. Ozone profile retrieval from recalibrated GOME data, *J. Geophys. Res.*, 107, 10.1029/2001JD000696 (2002).
4. Hasekamp O.P. and Landgraf J., Ozone profile retrieval from backscattered ultraviolet radiances: The inverse problem solved by regularization, *J. Geophys. Res.*, 106, 8077-8088 (2001).
5. Rodgers C.D., Inverse methods for atmospheric sounding: Theory and practice, ed. 1st. 2000, Singapore: World Scientific Publishing.
6. McPeters R.D., et al. Ozone climatological profiles for Version 8 TOMS and SBUV retrievals, *AGU 2003 Fall meeting*, San Francisco, California, 2003.
7. Chance K.V. and Spurr R.J.D., Ring effect studies: Rayleigh scattering, including molecular parameters for rotational Raman scattering, and the Fraunhofer spectrum, *Appl. Opt.*, 36, 5224-5230, 1997.

8. Sioris C.E. and Evans W.F.J., Impact of rotational Raman scattering in the O₂ A band, *Geophys. Res. Lett.*, 27, 4085-4088, 2000.
9. Chance K., Analysis of BrO measurements from the global ozone monitoring experiment, *Geophys. Res. Lett.*, 25, 3335-3338, 1998.
10. Schutgens N.A.J. and Stammes P., A novel approach to the polarization correction of spaceborne spectroscopy, *J. Geophys. Res.*, 108, 4229, doi:10.1029/2002JD002736 (2003).
11. Kurosu T.P., et al. CRAG-Cloud retrieval algorithm for ESA's GOME, *European Symposium on Atmospheric Measurements from Space*, 1999.
12. Bauman J.J., et al. Stratospheric aerosol climatology from SAGE II and CLAES measurements: 2. Results and comparisons, 1984-999, *J. Geophys. Res.*, 108, 4383, doi:10.1029/2002JD002993, 2003.
13. Martin R.V., et al. An improved retrieval of tropospheric nitrogen dioxide from GOME, *J. Geophys. Res.*, 107, 10.1029/2001JD001027, 2002.
14. Chance K.V., et al. Satellite measurements of atmospheric ozone profiles, including tropospheric ozone, from ultraviolet/visible measurements in the nadir geometry: a potential method to retrieve tropospheric ozone, *J. Quant. Spectrosc. Radiat. Transfer*, 57, 467-476, 1997.
15. Koelmeijer R.B.A., et al. A database of spectral surface reflectivity in the range 335-772 nm derived from 5.5 years of GOME observations, *J. Geophys. Res.*, 108, 2003.
16. Spurr R.J.D., et al. A linearized discrete ordinate radiative transfer model for atmospheric remote-sensing retrieval, *J. Quant. Spectrosc. Radiat. Transfer*, 68, 689-735, 2001.
17. Thompson A.M., et al. "Southern Hemisphere Additional Ozonesondes (SHADOZ) 1998-2000 tropical ozone climatology 1. Comparison with Total Ozone Mapping Spectrometer (TOMS) and ground-based measurements, *J. Geophys. Res.*, 108, 8238, doi:10.1029/2001JD000967, 2003.
18. Logan J.A., An analysis of ozonesonde data for the troposphere: Recommendations for testing 3-D models and development of a gridded climatology for tropospheric ozone, *J. Geophys. Res.*, 104, 16,115-16,149, 1999.
19. WMO, Scientific Assessment of Ozone Depletion: 1998. NASA, NOAA, UNEP, WMO, EC: Geneva, Switzerland. pp.1-44, 1999.
20. Thompson A.M., et al. Southern Hemisphere Additional Ozonesondes (SHADOZ) 1998-2000 tropical ozone climatology 2. Tropospheric variability and the zonal wave-one, *J. Geophys. Res.*, 108, 8241, doi:10.1029/2002JD002241, 2003.
21. Newchurch M.J., et al. Critical Assessment of TOMS-derived Tropospheric Ozone: Comparisons with Other Measurements and Model Evaluation of Controlling Processes. *Eos. Trans. AGU*, 82 (20), Spring Meet. Suppl. Abstract A52A-09, 2001.
22. Thompson A.M., et al. A Tropical Atlantic Paradox: Shipboard and Satellite Views of a Tropospheric Ozone Maximum and Wave-one in January-February 1999, *Geophys. Res. Lett.*, 27, 3317-3320, 2000.